Laser spectroscopy of the 1S-2S transition in hydrogen and deuterium: Determination of the 1S Lamb shift and the Rydberg constant

M. G. Boshier,* P. E. G. Baird, C. J. Foot, E. A. Hinds,† M. D. Plimmer,* D. N. Stacey, J. B. Swan,‡ D. A. Tate,§ D. M. Warrington,** and G. K. Woodgate
Clarendon Laboratory, University of Oxford, Parks Road, Oxford OX1 3PU, United Kingdom
(Received 12 June 1989)

We have observed the narrow 1S-2S transition in hydrogen and deuterium with high resolution using Doppler-free two-photon absorption of continuous-wave 243-nm light. The transition frequencies were measured by direct comparison with accurately calibrated lines in the spectrum of the $^{130}Te_2$ molecule. We find the 1S-2S interval to be 2 466 061 414.1(8) MHz in hydrogen and 2 466 732 408.5(7) MHz in deuterium. By combining these results with recent measurements of the Rydberg constant we obtain the values 8172.6(7) and 8183.7(6) MHz for the 1S Lamb shifts in hydrogen and deuterium, respectively. These are the most precise measurements of the 1S Lamb shifts in these atoms and they are in excellent agreement with the theoretical values of 8173.03(9) and 8184.08(12) MHz. Alternatively, if the 1S Lamb shift is supposed known from theory, our measurements determine the Rydberg constant as $R_\infty = 109\,737.315\,73(3)\ \mathrm{cm}^{-1}$.

I. INTRODUCTION

In this paper we describe a precise measurement of the frequency of the 1S-2S transition in atomic hydrogen. This transition has attracted much attention because its extremely small natural width (1.3 Hz) makes possible precise tests of bound-state quantum electrodynamics (QED) by the method of two-photon spectroscopy.[1] In particular, with this method it should be possible to surpass the precision of radio-frequency spectroscopy measurements of the $2S_{1/2}$-$2P_{1/2}$ Lamb shift[2,3] which are now reaching the fundamental limit imposed by the 100-MHz natural width of the $2P_{1/2}$ level. Spectroscopy of the 1S-2S transition can also lead to more accurate values for fundamental constants.

A potential difficulty in using the 1S-2S transition to study QED effects arises because the Lamb shifts make up only a tiny part of the total interval—about 7 GHz, compared to the Dirac energy of 2.5×10^6 GHz. This problem was avoided in the first experiments on the 1S-2S transition, at Stanford,[4] in which the 243-nm light required to excite the two-photon transition was generated by frequency doubling. When the 243-nm light is resonant with the 1S-2S transition the fundamental radiation (at 486 nm) is close to resonance with the $n=2$ to $n=4$ Balmer-β transition. In the nonrelativistic Bohr approximation the coincidence would be exact. The detuning from resonance on Balmer β is due to relativistic and hyperfine corrections, all of which are well understood, and the Lamb shifts, which are thus determined by the measurement.

The 243-nm light was generated by frequency doubling because there are no laser sources of light at this wavelength. The nonlinear optical mixing, in combination with the two-photon absorption, leads to a very nonlinear dependence of transition rate on fundamental laser power, so it was natural that early work on the 1S-2S transition used high-power pulsed 243-nm light sources.[5–8] The precision of those experiments was limited by frequency shifts in the pulsed dye amplifiers and by the large linewidths of the pulsed sources. Considerable effort has therefore been put into the development of continuous-wave (cw) 243-nm sources because they are free of the frequency chirping problem and have a narrow linewidth.

A cw 243-nm source using sum-frequency mixing of an ultraviolet (uv) ion laser and a red dye laser was developed at Stanford University.[9] Recently, the 1S-2S transition in hydrogen was observed[9] using this source and its frequency was measured.[10] By using an accurate value of the Rydberg constant it was possible to extract the Lamb shift. This calibration procedure is essentially the same comparison of hydrogen transitions used in the early experiments, but with several intermediate steps linking the two transitions.

Our work at Oxford University[11] has concentrated on the development of frequency doubling as a means of generating cw 243-nm light because it offers the long-term prospect of a direct comparison of the 1S-2S and Balmer-β transitions. In this paper we describe the first experiment on hydrogen 1S-2S using cw 243-nm light generated by frequency doubling.[12,13] We have measured the 1S-2S transition frequency $f(1S\text{-}2S)$ in both hydrogen and deuterium. As in Ref. 9 our determination of the Lamb shift uses an indirect calibration via the Rydberg constant; however, the use of frequency doubling reduces the number of intermediate steps and by employing two lasers it was possible to calibrate the measurement using accurate heterodyne techniques. These improvements lead to a value of the hydrogen 1S Lamb shift which is a factor of 3 more precise than the previous value, and to the first cw measurement of the 1S Lamb shift in deuterium, improving the precision in this case by a factor of 50. An alternative interpretation of our measurements is pos-

sible if the $1S$ Lamb shifts are assumed known from theory; the work then furnishes a new value of the Rydberg constant.

II. BACKGROUND

A. 1S Lamb shift in hydrogen

Neglecting hyperfine structure, one can express the energy levels of hydrogenic atoms in the form

$$E(n,j,l)=E_D(n,j)+E_{\rm rel}(n)+E_L(n,j,l) , \tag{1}$$

where $E_D(n,j)$ is the Dirac energy and the correction $E_{\rm rel}(n)$ is required because the relativistic two-body problem does not reduce exactly to an equivalent reduced mass single-particle problem. It is given approximately by[14]

$$E_{\rm rel}(n)=-\frac{\mu}{M+m}\frac{\alpha^2}{4}\frac{Z^4}{n^4}\frac{\mu}{m}{\rm Ry} , \tag{2}$$

where m and M are the electronic and nuclear masses, μ is the reduced mass, Z is the nuclear charge in units of the elementary charge, α is the fine-structure constant and Ry is the rydberg. The last term in (1), $E_L(n,j,l)$, is the Lamb shift, made up of QED corrections and a correction for the finite size of the nucleus.

Comprehensive reviews of contributions to the Lamb shift in hydrogenic atoms have been given by Erickson[14] and by Johnson and Soff.[15] The theoretical value for the $1S$ Lamb shift given in this paper is based on the results of Johnson and Soff, including Mohr's numerical calculation of some binding corrections to self-energy and vacuum polarization.[16] We also include the additional recoil corrections calculated by Bhatt and Grotch[17] and by Erickson and Grotch,[18] and we apply the reduced mass factor $(\mu/m)^3$ to the binding corrections to self-energy and vacuum polarization. The expression obtained in this way is consistent with that given by Erickson and Grotch. The results are 8173.03(9) MHZ for hydrogen and 8184.08(12) MHz for deuterium. We have used charge radii of 0.862(12) fm and 2.116(12) fm for the proton[19] and the deuteron.[20] If the earlier measurement[14] of 0.80(2) fm for the proton charge radius is used the calculated $1S$ Lamb shift for hydrogen becomes 8172.87(10) MHz. The present experiment does not distinguish between these two values. The uncertainty in the calculated hydrogen $1S$ Lamb shift arises from the following contributions: uncertainty in the numerical estimate of binding corrections 73 kHz; proton charge radius 33 kHz; uncalculated QED corrections 45 kHz.

B. Two-photon spectroscopy of hydrogen 1S-2S

The generation of sufficient 243-nm radiation is a critical part of a cw $1S$-$2S$ experiment; we review briefly the theory of two-photon absorption as it applies to hydrogen $1S$-$2S$ in order to estimate the power required.

The $1S$-$2S$ transition rate for a hydrogen atom in counterpropagating 243-nm fields with amplitude $\mathcal{E}$, frequency ω, and polarization vector ϵ is given by second-order time-dependent perturbation theory as[21,22]

$$\mathcal{R}=\frac{\mathcal{E}^4}{4\hbar^4}|M|^2 2\pi g(\omega) , \tag{3}$$

where

$$M=\sum_j \frac{\langle 1S|e\mathbf{r}\cdot\boldsymbol{\epsilon}|j\rangle\langle j|e\mathbf{r}\cdot\boldsymbol{\epsilon}|2s\rangle}{\omega_{j1s}-\omega} , \tag{4}$$

and $g(\omega)$ is a normalized line-shape function given for our case by a Lorentzian profile of full width at half maximum (FWHM) Γ_{2s},

$$g(\omega)=\frac{1}{\pi}\frac{\Gamma_{2s}/2}{(\omega_0-2\omega)^2+\Gamma_{2s}^2/4} . \tag{5}$$

In these equations $\omega_j=E_j/\hbar$, where E_j is the energy of level j, $\omega_{j1s}=\omega_j-\omega_{1s}$, and $\omega_0=\omega_{2s}-\omega_{1s}$. The summation in (4) of dipole matrix elements over all intermediate states including the continuum has been carried out by Bassani *et al.*[23] For $\omega=\omega_0/2$ they calculated the dimensionless quantity

$$D[J_0]=\frac{6\pi cR_\infty}{e^2a_0^2}M \tag{6}$$

to be -11.78, giving $M=-1.36\times10^{-74}$ C^{2}m^{2}s. We consider ground-state hydrogen atoms in a cell with number density N excited by counterpropagating beams, each of total power P and waist radius w. If the excitation is monitored over a length L which is small compared to the Rayleigh length of the beam, as in the present experiment, the total excitation rate in the detection volume is given by

$$r=(6.81\times10^{-8}\ {\rm W^{-2}m^4s^{-1}})\frac{LNP^2}{w^2}g(\omega)\ {\rm s^{-1}} . \tag{7}$$

The experimental parameters were chosen as follows. Focusing the beam to a smaller waist size increases the two-photon excitation rate, but it also increases the broadening of the resonance by the finite transit time of atoms through the beam. The transit-time broadening corresponding to a waist size of 100 μm is about 4 MHz (at the atomic frequency), which was similar to the contribution from the laser bandwidth. Gas pressures of around 0.1 torr are required to limit pressure broadening to a few megahertz. The total width $\Gamma_{2s}/2\pi$ would therefore be about 10 MHz and the atomic number density would be about 3×10^{21} m^{-3} if the gas were completely dissociated. The two-photon excitation can typically be observed over a length of 1 cm with an overall detection efficiency of 0.1%. The signal size on resonance is therefore expected to be about $10^{10}P^2$ W^{-2}s^{-1}. In earlier experiments where the resonance was also excited in a cell[5] it was noted that the observed signal was up to three orders of magnitude less than expected, probably due to the combined effects of incomplete dissociation, radiation trapping, and nonradiative quenching.[24] Taking this factor into account, it is clear that a few milliwatts of 243-nm radiation are required to produce an observable resonance signal of about 10 s^{-1}.

Selection rules for two-photon transitions have been considered by Grynberg and Cagnac.[25] In this experiment the selection rules for the total angular momentum

F and its projection m_F are $\Delta F=0$ and $\Delta m_F=0$. The $1S$-$2S$ two-photon line thus has two components with intensity ratios determined by the level degeneracies, i.e., 3:1 for hydrogen and 2:1 for deuterium.

III. EXPERIMENTAL APPARATUS

A. Overview

The apparatus (Fig. 1) has two major parts, the two-photon $1S$-$2S$ spectrometer and the frequency-calibrating tellurium spectrometer, each based on a 486-nm ring dye laser (Coherent Radiation CR699-21 using coumarin 102 dye) pumped by the all-lines violet output of a krypton ion laser (Coherent Radiation Innova K3). The 243-nm light required for exciting the $1S$-$2S$ transition was generated by intracavity frequency doubling in ring dye laser 2 and then focused into an enhancement cavity which contained ground-state hydrogen atoms. The two-photon spectrum was calibrated with respect to dye laser 1 which was servo-locked to accurately measured lines in the spectrum of $^{130}Te_2$. The difference frequency was measured precisely by heterodyning the 486-nm outputs of the two lasers together on a fast photodiode and measuring the beat frequency with a microwave frequency counter.

B. Generation of cw 243-cm light

Generation of 243-nm light by frequency doubling has been very difficult until recently because of the lack of a suitable nonlinear crystal. Our early work[11] used lithium formate monohydrate (LFM), but this proved inadequate for the hydrogen experiment because of the poor efficiency of LFM and because of damage to the crystal induced by the generated uv light. Better results were obtained with urea, especially after it became possible to polish the crystal surfaces well enough to dispense with an index-matching fluid. Although urea also suffers from uv-induced damage, this was confined to the surfaces and we were able to make the initial observation and preliminary measurements of the $1S$-$2S$ transition using it. Considerable effort was put into the optimization of the system with LFM and urea; this involved taking account of the crystal optical quality and describing and correcting for the elongation of the uv beam intensity profile which results from Poynting vector walkoff.

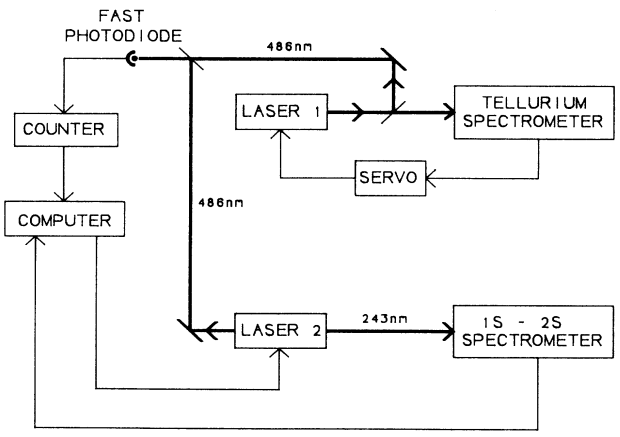

FIG. 1. Schematic diagram of the overall layout.

The results reported here have been obtained using the new nonlinear material β-barium borate (BBO).[26,27] This crystal is superior to urea in almost all respects: BBO is hard, has good optical quality, and can be polished well. It provides good conversion efficiency and, most important, does not suffer from any uv-induced damage. The crystal used (supplied by the Fujian Institute of Research on the Structure of Matter, Fujian, China) was a Brewster-cut rhomb 7 mm thick with 7×4 mm^2 entrance and exit faces, cut so that $\theta=59.2°$ and $\phi=0°$ in the notation of Ref. 27. The modifications made to the Coherent 699-21 ring dye laser for frequency doubling are described elsewhere.[11] The crystal was mounted in a sealed cell with thick quartz windows and type-I phase matching was achieved by angle tuning about the normal to the crystal entrance and exit faces. With 5 W of violet output from the pump laser, it was possible to routinely generate 3 mW of stable, single-frequency light at 243 nm with a bandwidth of less than 2 MHz. A detailed account of the use of these three materials for generating cw 243-nm radiation can be found in Ref. 13.

The laser was frequency scanned smoothly over the narrow (2 MHz) $1S$-$2S$ resonance by moving the lock point of the frequency servo-control up and down the side of a reference cavity transmission fringe. The reference cavity was also enclosed in a cardboard shield to exclude draughts. This arrangement gave smoother scans than were possible using the galvanometer-mounted plate in the reference cavity and improved the laser frequency stability by leaving the reference cavity undisturbed. The frequency scan is slightly nonlinear but this was not important here because the heterodyne calibration provided a frequency measurement at every point in the scan, removing any need for interpolation.

C. $1S$-$2S$ spectrometer

Figure 2 is a schematic diagram of the $1S$-$2S$ spectrometer. In this system hydrogen atoms were produced in a discharge dissociator and flowed along a Teflon pipe into the interaction cell. This cell formed part of an optical cavity that enhanced the intensity of the 243-nm light from the frequency-doubled laser. The two-photon excitation to the $2S_{1/2}$ level was detected by monitoring 122-nm Lyman-α photons emitted after collisional transfer to the $2P_{1/2}$ level.[5]

1. Hydrogen Source

The source consisted of a Pyrex discharge tube placed inside a helical radio-frequency (rf) resonator.[28] The resonator design followed the analysis presented by MacAlpine and Schildknecht.[29] About 50 W of radio-frequency power at a frequency of 29 MHz (provided by a Heathkit DX-100U amateur radio transmitter) was

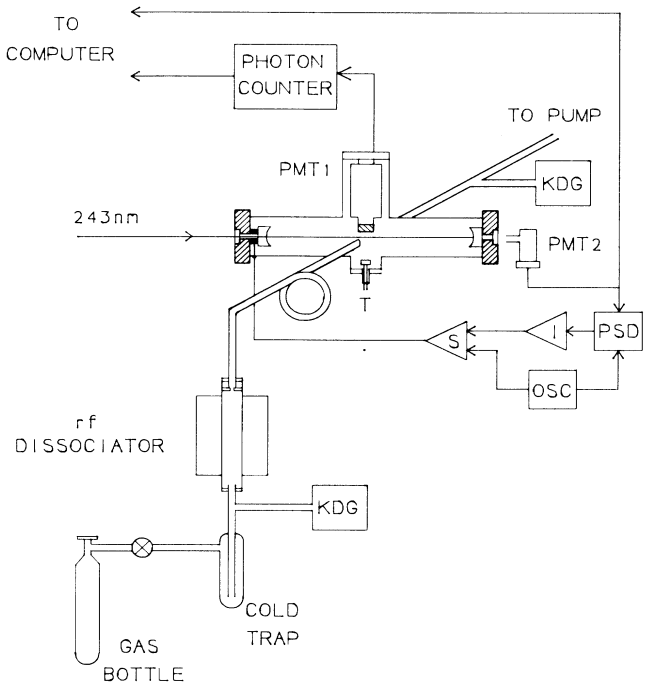

FIG. 2. Schematic diagram of the $1S$-$2S$ spectrometer. PMT1, Lyman-α sensitive photomultiplier; PMT2, 243 nm-sensitive photomultiplier; KDG, manometer, T, Thermoflake atomic hydrogen detector; PSD, phase-sensitive detector; OSC, 20-kHz oscillator; I, integrator; S, summing amplifier.

coupled into the resonator through a single loop of copper tube placed around the coil near the short-circuited end.

The Pyrex dissociator tube (12 mm diameter) was cooled with compressed air because the dissociation fraction decreased if the tube walls became too hot. The atomic hydrogen concentration was also found to be very sensitive to contamination of the tube walls, so a liquid-nitrogen-cooled cold trap was incorporated in the gas line between the gas bottle and the dissociator. The dissociator tube had a short constriction with a 3-mm diameter aperture near the downstream end. The discharge was run right up to this constriction, and a ~ 30 cm length of Teflon tube was butted up against the other side of it. Teflon was used because it has a low surface recombination rate for atomic hydrogen.[30] This arrangement kept the amount of Pyrex in the flow path to a minimum, while preventing the discharge from attacking the Teflon tube. The Teflon tube was bent into a loop to prevent Lyman-α light from the discharge from striking the photomultiplier, and reached into the interaction region through a side arm on the cell. A KDG inductance manometer (model 4010/P3/A/X2/44, range 0–20 torr) was coupled to the dissociator tube to measure the pressure in the discharge. Pressures in the range 0.1 to 1.2 torr were used during the experiment. The flowing system was pumped with a four-inch oil diffusion pump with a liquid-nitrogen cold trap. A needle valve on the gas bottle served to limit the total flow.

While the radio-frequency discharge gave almost complete dissociation—no trace of the molecular lines was seen when the discharge fluorescence was viewed through a spectrometer— it is much harder to estimate the density of atomic hydrogen in the interaction region. Walraven and Silvera[31] have demonstrated that hydrogen gas at a density of 6×10^{20} m^{-3} can be transported down a 25 cm long Teflon transport tube and emerge with a dissociation fraction of 60%. However, since the densities in our experiment were somewhat higher than this and the transport tube was coupled directly into the enhancement cavity, which contained many metal parts, recombination was probably more severe in our case. A lower bound of 0.1% can be placed on the dissociation fraction from the fact that the observed two-photon signal intensity was about 10^{-3} of that calculated assuming that dissociation was complete and that every excitation gave rise to a detectable Lyman-α photon.

2. *Interaction Region*

The cell was constructed from a 35 cm length of 4.5 cm diameter Pyrex tube with central horizontal side arms for gas entry and exit. A second KDG manometer was attached to the exit side arm to measure the pressure in the cell. The Lyman-α fluorescence was detected by a photomultiplier which was mounted vertically above the interaction region.

A Thermoflake (Thermometrics No. A500-2F40M105Q) was mounted just below the interaction region in a third side arm. The Thermoflake is a flake thermistor whose resistance has been found to be very sensitive to the concentration of atomic hydrogen.[32] Although the response of the flakes was sensitive to contamination and different flakes often exhibited different behavior they still provided a useful indication of the hydrogen density in the cell.

The cell formed part of an optical enhancement cavity which performed several functions: it enhanced the intensity of the 243-nm radiation by a factor of 12, it provided the standing-wave field required for the Doppler-free two-photon absorption, and it enabled the forward- and backward-traveling beams to be accurately overlapped. The optical configuration of the cavity was determined by several considerations. Firstly, a waist size of around 100 μm was required to obtain a large two-photon transition rate without excessive transit-time broadening. Secondly, nonconfocal mirror separation was required to ensure that the waist of the cavity mode was located at the center of the cavity, underneath the photomultiplier. Thirdly, it was desirable to have the cavity linewidth a little larger than the bandwidth of the 243-nm light (~ 2 MHz) so that the cavity would not be thrown out of lock by laser frequency fluctuations. These constraints were satisfied by building a cavity with two mirrors with radius of curvature 30 cm placed 49 cm apart, giving a waist size for the TEM_{00} fundamental mode of 95 μm at 243 nm. The input coupler reflectivity was 94% and that of the cavity end mirror 98%. The mirror mounts sealed directly onto the ends of the cell via flexible metal bellows and were rigidly located with four

Invar bars. This design removed the need for intracavity cell windows that we had previously found to reduce the enhancement factor and increase the amount of scattered light. Draughts were also excluded, improving the passive stability of the cavity. The input coupler was mounted on a small disk of piezoelectric (PZT) ceramic and modulated at 20 kHz to enable the cavity to be locked in resonance with the 243-nm light using standard phase-sensitive detection techniques. A uv-enhanced photomultiplier (Hamamatsu R-166) was mounted behind the weakly-transmitting cavity end mirror to monitor the intracavity power and provide an error signal.

One of the disadvantages of using angle-tuned second-harmonic generation is that the frequency-doubled beam has an elongated intensity profile due to Poynting vector walkoff.[33] Some care is therefore necessary to mode match this beam efficiently into the cylindrically symmetric geometry of the enhancement cavity. This problem is particularly severe in the case of BBO because of its large birefringence. In the limit of weak focusing the uv beam has an approximately rectangular intensity profile in the walkoff direction.[34] We constructed an optical system consisting of a cylindrical lens and a spherical lens designed to optimize the overlap of this rectangular uv beam with the cavity mode. A theoretical model for BBO predicted that it should be possible to couple in 88% of the second-harmonic power in this way, compared with only 7% for a system restricted to just spherical lenses (the aspect ratio of the beam is about 20:1 in the far field for the BBO system). The actual mode-matching efficiency could not be measured directly because it could not be separated from measurement of the cavity enhancement factor. The total enhancement factor was measured to be 12, compared with the maximum value of 37 theoretically possible with the mirror reflectivities used, placing a lower bound on the coupling efficiency of 30%.

The Lyman-α detection system comprised a solar blind photomultiplier tube (EMI G26L314LF) with a quantum efficiency of 10% at 121.6 nm and a Lyman-α interference filter (Acton Research Corp., Model 122-N), mounted just above the interaction region. The photomultiplier subtended a solid angle of 0.06 sr and the interference filter had a transmission of 23%, giving an overall detection efficiency of 1.4×10^{-3}. The photomultiplier output was connected to a pulse counter via a pulse amplifier and discriminator. The photomultiplier was operated with a grounded photocathode and positive polarity high-voltage bias in order to avoid electric fields in the cell which could have produced Stark shifts. Scattered 243-nm light detected by the Lyman-α photomultiplier was found to be responsible for effectively all the background in the $1S$-$2S$ spectra; the quantum efficiency was found to be 0.01% at this wavelength. Four baffles were therefore installed along the optical axis of the cell, reducing the background to a sufficiently low level of about $100\ s^{-1}$ per milliwatt of 243-nm power inside the cavity.

D. Tellurium reference spectrometer

Figure 3 is a schematic diagram of the tellurium reference spectrometer. The major concern in this part of the

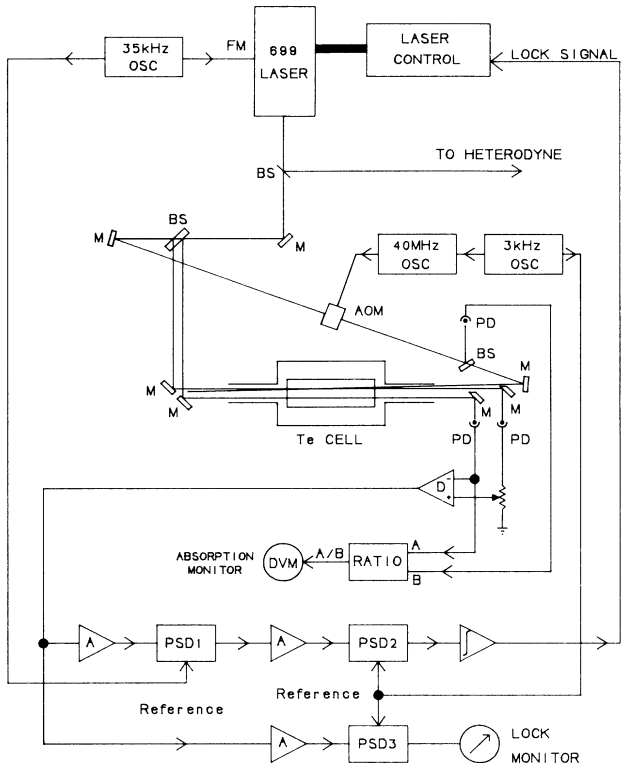

FIG. 3. Schematic diagram of the tellurium spectrometer. BS, beamsplitter; *M*, mirror; PD, photodiode; *D*, differential amplifier; OSC, oscillator; PSD, phase-sensitive detector; *A*, amplifier; *I*, integrator; DVM, digital voltmeter.

experiment was to reproduce as closely as possible the conditions of the original frequency calibration made at the National Physical Laboratory (NPL) in England.[35] For the hydrogen (deuterium) scans the reference laser was locked to the line designated b_2 (b_1) in Ref. 35. The linewidths of these transitions in our spectrometer were about 20 MHz for b_2 and 14 MHz for b_1.

1. Reference dye laser

Because only a small amount of power was required for the tellurium spectrometer, the reference laser was operated in a standing-wave configuration. This reduced the pumping threshold considerably and extended the dye lifetime. The dye laser was also significantly more stable in the standing-wave configuration.

The dye laser was locked to its standard reference cavity, providing good short-term stability (a linewidth of ~ 1 MHz). The slower fluctuations of the reference cavity were mostly removed by a servo-loop that kept the laser frequency resonant with the calibrated tellurium transition. The dye laser was frequency modulated so that the derivative of the tellurium lineshape could be obtained, and the laser frequency was locked to the zero crossing of this curve using standard techniques. The laser was frequency modulated at 35.4 kHz (to a depth of 5 MHz

peak-to-peak) by directly driving a mechanical resonance of the small PZT-mounted laser cavity mirror (the "tweeter") at this frequency. The modulation was coupled in through a transformer connected in series with the tweeter. The use of a relatively high modulation frequency improved the signal-to-noise ratio because the amplitude of the laser intensity fluctuations, the main source of noise, falls off towards higher frequency. The error signal was fed back to the laser via the External Scan input of the control box.

2. *Saturated absorption spectrometer*

The probe and pump beams in the saturated absorption spectrometer were made as close to collinear as possible without having the back reflection of the pump beam from the laser output coupler directed back into the spectrometer. A reference probe beam and a differential amplifier were used to reduce the effects of laser intensity fluctuations. The 35-kHz frequency modulation of the laser under the transmission curve of the intracavity thick étalon resulted in a small ($<0.5\%$) synchronous amplitude modulation at the same frequency. This was not completely removed by the differential amplifier, because it proved impossible to maintain the differential amplifier null as the beams moved. This residual intensity modulation was demodulated in the first phase-sensitive detector (PSD1), forming a background which changed with time as the alignment drifted. The background was removed by chopping the pump beam at 3 kHz and adding a second phase-sensitive detector (PSD2) to isolate the signal components that depended on the pump beam intensity. There remained a small additional effect because the saturated absorption signal depends on the intensities of the probe and pump beams; this is discussed below. The additional modulation on the pump beam necessary to remove the amplitude modulation background was applied with an acousto-optic modulator (Intra-Action AOM-40 driven by a Marconi 2019A frequency synthesizer and a Mini-Circuits ZHL-1A power amplifier) which chopped the beam at 3 kHz and upshifted it in frequency by 40 MHz. The probe beams had a power of 2 mW each and were focused to a waist of 330 μm in the cell. The pump beam (power 10 mW) was focused to the larger spot size of 670 μm in the cell to reduce the effects of beam movement.

A third phase-sensitive detector (PSD3) was included to detect a normal saturated absorption signal using only the pump beam modulation signal. This was used to monitor the lock during the data collection. Finally, the absorption of a weak probe beam in the cell was monitored by dividing (in an analog ratiometer) the output from the reference probe beam photodiode by the output from a third photodiode monitoring the pump beam intensity.

3. *Tellurium Cells*

Two tellurium cells were used in this experiment. A cell which was nominally a duplicate of the one calibrated at NPL was used for preliminary investigations of systematic errors in the tellurium spectrometer. This duplicate cell was mounted in a fire-brick oven heated with "clam-shell" heater elements, and a thermostatic temperature control was used. The initial $1S$-$2S$ spectra were calibrated against the duplicate cell; all of these spectra gave values for the Lamb shift below that of Beausoleil *et al.*[10] and below the theoretical value by approximately 1 MHz (at 486 nm). We then obtained the actual cell calibrated at the NPL. $1S$-$2S$ spectra calibrated against the NPL cell revealed that there was indeed a difference of ~ 1 MHz (at 486 nm) in the frequency of the b_2 line observed in the two cells. This is obviously a very serious problem for a secondary frequency standard.

We initially thought that the NPL cell was suspect, because the published saturation spectra (Fig. 2 in Ref. 35) looked quite different to the spectra obtained both with our duplicate cell and with a similar cell at Stanford.[36] The linewidths reported also disagreed significantly: a value of 34(3) MHz was found for the b_2 line at NPL, compared with 24(2) MHz from our preliminary measurements and a value of 20.2(9) MHz from the Stanford work. These results would be consistent with the presence of a foreign gas in the NPL cell, which would, of course, render it useless as a frequency standard because one could not be certain that the cell conditions were not changing with time. However, saturation spectra of the region around the b_2 line taken with the NPL cell in our own spectrometer are almost identical to our earlier results and to those obtained at Stanford. Further, we measured the linewidth of the b_2 line in the NPL cell as 20(2) MHz, the same as the Stanford value. It is very unlikely that the linewidth had become narrower with time, so we concluded that the measurement of the linewidth made during the experiments preliminary to the NPL calibration overestimates it considerably, and that the cell was actually still the same as it was when it was calibrated. For this reason, we have used the NPL cell to calibrate all the results presented here. Several months after finishing the collection of the $1S$-$2S$ data it was found that a Tesla coil brought near to our duplicate cell caused a faint discharge inside it, suggesting that it had indeed become contaminated in some way. No firm conclusions can be drawn from the slightly larger linewidth found in our earlier measurements on the duplicate cell since at that time narrow linewidths were not of prime importance and the residual Doppler shift could have amounted to a few megahertz. In view of these results it would seem advisable to employ at least two cells in any future measurements that rely on the tellurium lines for frequency calibration.

In using the NPL cell we followed the procedure recommended by Barr *et al.*[35] of bringing the cell up to the operating temperature slowly to avoid overheating the cell and possible outgassing. The NPL cell was heated with the apparatus used in the original calibration, except that metal tubes were fixed to each end of the box containing the cell to shield the windows from draughts. The cell temperature was monitored with a thermocouple and controlled by manual adjustment of the Variac supplying the heater current.

There has been some confusion about the correct

operating temperature for the tellurium cells.[7] The original calibration quoted a cold-point temperature of 625(6) °C for the conditions of the measurement.[35] The absorption of a low power beam on an isolated line ~9 GHz below the b_2 line was also recorded [23(2)% under the calibration conditions], providing a more reliable measure of the vapor pressure in the cell. The Stanford workers claim that this absorption corresponds to a cold-point temperature of 513 °C.[7] We have recorded spectra of the calibrated region under the standard conditions and find that the Dopper width of the isolated line is 780 MHz, which implies a vapor temperature of ~540 °C. This is obviously incompatible with the NPL measurement of the cold-point temperature. Therefore we have relied on the unsaturated linear absorption (measured using an analog ratiometer) on the isolated line as a measure of the vapor pressure in all of the results presented here.

In an auxiliary series of experiments tellurium spectra were recorded over a wide range of temperatures, with a frequency calibration provided by two stable confocal interferometers of free spectral ranges 75 and 375 MHz. These spectra were linearized and the frequency of the b_2 line found by taking a center of gravity. The linear absorption was also recorded so it was possible to determine the pressure shift as a function of the absorption length on b_2 and on the strong single line. The absorption was then measured as a function of the temperature indicated by the thermocouple attached to the NPL cell (the thermocouple was used to monitor the cell temperature after the temperature had been set from the absorption). From these data we obtained the following measure of the pressure shift of the b_2 line as a function of the thermocouple reading and of the absorption length on the strong single line (at the normal operating temperature): a 3 °C change in temperature changes the linear absorption by 2% and shifts the b_2 line by 40 kHz. During the data collection the manual control of the cell temperature limited temperature excursions to ±4 °C.

E. Frequency calibration

The 1S-2S spectrum was calibrated by heterodyning 486-nm light from the scanning frequency-doubled laser with light from the locked reference laser. This heterodyne scheme, which, of course, requires two laser systems, offers the advantages of precision and freedom from the need for interpolation.

A few milliwatts of 486-nm light from each dye laser were combined by a beamsplitter and focused onto a fast avalanche photodiode (AEG-Telefunken BPW 28). The photodiode was mounted in a holder designed to match the impedance of the diode to that of a 50-Ω semirigid coaxial cable.[37] The resulting beat signal (~1400 MHz for H-b_2 and ~4200 MHz for D-b_1) was amplified by 30 dB in a microwave amplifier (Mini-Circuits ZHL-42) and measured with a microwave frequency counter (Hewlett-Packard HP 5343 A).

The accuracy of the 1S-2S transition frequency measurement depended critically on this part of the experiment, so the performance of the heterodyne system was carefully checked. Firstly, the laser output was passed through an acoustic-optic modulator (AOM) to make a 40-MHz sideband which was then heterodyned against the unshifted laser output. The result was consistently 39 999 970(20) Hz. This confirmed the accuracy of both the frequency synthesizer used to drive the AOM and the microwave counter, and also indicated that the microwave counter was able to "flywheel" over any intensity fluctuations in the laser output caused by bubbles passing through the dye jet. Furthermore, with the two lasers heterodyned together we confirmed that there was no change in beat frequency when the frequency modulation was applied to the reference laser. Finally, the statistical distribution of the beat frequencies measured between the two lasers was checked. To do this 1000 sequential beat measurements were recorded and a moving average was used to subtract off the slow drifts of the lasers on a time scale of more than a few seconds. No statistically significant discrepancy between the actual distribution of beat measurements and a normal distribution with the same mean and standard deviation was found.

F. Computer control system

The operation of the experiment and the data collection were controlled by a small microcomputer (IBM PC). The microwave frequency counter and the counter-timer (Phillips PM6671) used to count the Lyman-α photons communicated with the computer via an IEEE-488 interface. The computer was fitted with a Tecmar LabMaster data acquisition board which incorporated 12-bit analog-to-digital converters (ADC's), 12-bit digital-to-analog converters (DAC's) and programmable counters. The counters were used in conjunction with a 1-MHz crystal oscillator on the LabMaster board to control the timing of the data collection and the gating of the photon counter. A DAC was used to scan the frequency-doubled dye laser. The uv intensity in the enhancement cavity was time averaged with a 100-ms linear averaging filter and then recorded via one of the ADC's.

G. Data collection procedure

Typical scans made with this system contained 100 points with a 1-s sampling time at each point, covering a total frequency range of 20–30 MHz. The beat frequency was measured nine times during each 1-s sampling period, and all of these values, along with the average beat frequency and the Lyman-α photon count, were recorded at each point. The uv power inside the enhancement cavity was also recorded at each point since it varied across the scan. The scan direction was reversed (up and down in frequency) for successive scans as a precaution against possible systematic error, though none was found in the analysis.

Collisions between atomic and molecular hydrogen result in a significant pressure shift of the 1S-2S transition. Scans were therefore recorded down to very low cell pressures, so that an accurate extrapolation could be made to zero pressure. As a further check on this systematic uncertainty, runs were also taken with the pure hydrogen or

deuterium replaced by a dilute mixture of hydrogen and deuterium in helium. A similar mixture was used in the cw Stanford experiments[10] because it was found to give a smaller pressure shift, presumably as a result of the small polarizability of the helium atom.[38] A complete data set consisted of about six successive scans at each of four to six different pressures in the range 20–300 mtorr. Data collection alternated between high and low pressures within this range, to reduce the effect of any systematic sources of error with a slow time dependence. Although each scan only lasted 100 s, the collection of data at a given pressure took considerably longer (~2000 s), because the lasers and various servo loops required frequent attention. Thus, the time taken to collect a complete data set was of the order of a few hours.

In all of the work presented here, the scans were made over the stronger of the two hyperfine components of the $1S$-$2S$ transitions, i.e., $F=1\rightarrow F'=1$ for hydrogen and $F=\frac{3}{2}\rightarrow F'=\frac{3}{2}$ for deuterium.

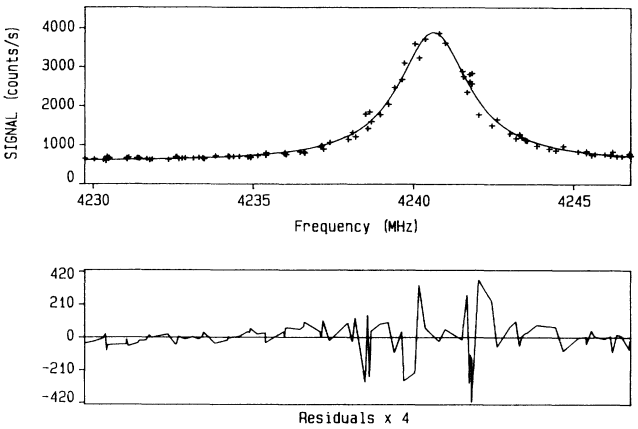

FIG. 4. Typical $1S$-$2S$ spectrum. The crosses are data points and the solid line is the best least-squares fit of the line shape discussed in the text. The lower graph shows the difference between the fitted curve and the data magnified by a factor of 4. The signal is the number of Lyman-α photons detected per second and the frequency is measured relative to the tellurium b_1 line. This is the $F=\frac{3}{2}\rightarrow F'=\frac{3}{2}$ component of deuterium $1S$-$2S$, recorded with 0.2 torr of the helium mixture in the cell.

IV. ANALYSIS AND RESULTS

A. Analysis

1. *Curve fitting*

The center frequency and linewidth of each run were found by fitting the scan to a theoretical line shape. The fitting program was based on a FORTRAN implementation of the Levenberg-Marquardt method for finding the best least-squares fit described by Press *et al.*[39] In preliminary experiments it was determined that the background was entirely due to scattered 243-nm light, so the theoretical line shape used was a Lorentzian profile superimposed on a scattered light background which was assumed to be linearly proportional to the uv power. The Lorentzian amplitude was taken to be proportional to the square of the recorded intracavity 243-nm power. An additional parameter describing a quadratic intensity response of the photomultiplier was included to take account of a slight nonlinearity in the uv power measurement. All five fitting parameters (resonance frequency, linewidth, height, background size, and nonlinearity) were allowed to float in the fit.

Figure 4 shows the fit of this profile to a $1S$-$2S$ scan. In the wings of the line the residuals (the difference between the experimental data and the best-fit profile) are roughly equal to the square root of the number of photons detected. This is the limit expected from statistical fluctuations, so we can be confident that the uv intensity normalization is adequate. We believe that the hydrogen number density is constant over the time taken to scan several points (a few seconds) so we conclude that most of the noise on the resonance above the statistical contribution is actually due to frequency fluctuations of the reference laser; if this moves in frequency, then an error is introduced into the beat frequency recorded. Frequency variations of the $1S$-$2S$ spectrometer laser are less important, since although they change the photon count rate the heterodyne signal changes correspondingly. The fluctuations of the reference laser are of two types: relatively fast (above a few hertz) fluctuations of the laser reference cavity that are not completely corrected by the servo, and the considerably slower (~300 s) thermal drift of the tellurium cell (discussed in Sec. III D 3). We are concerned with the fast fluctuations here. The slower movements are actually the major cause of the scatter in the results of individual runs, but it will be seen that they make only a small contribution to the final uncertainty.

We checked that the fast fluctuations of the reference laser frequency averaged to zero over the time taken to scan across the $1S$-$2S$ profile (~20 s) by smoothing the frequency scale with a seven-point moving average (replacing each point by the average of itself and the three neighboring points on each side) and fitting the line again. The quality of the fit was improved by this procedure, indicating that the fluctuations did indeed average out. It is straightforward to show that the application of a moving average to our nonlinear frequency scan results in a systematic frequency shift (~50 kHz in this case), so the smoothing was not used in determining the resonance frequency. In most cases the difference between the smoothed and unsmoothed fits was fairly close to 50 kHz. However, on four runs the difference was much larger (~400 kHz); the fits were relatively poor, and the beat frequencies recorded in these scans were all found to exhibit jumps of several megahertz. The data from these runs were therefore rejected.

2. *Description of the data set*

Details of the data sets are given in Table I. The first complete set of runs used pure hydrogen gas (set 1, 26 scans). A similar set using pure deuterium was then taken (set 2, 27 scans). Both sets give excellent fits to a

TABLE I. Results of the data reduction. All frequencies are measured at 486 nm.

Data set	Number of scans	Gas mixture	Zero-pressure offset frequency (MHz)	Pressure shift (MHz/torr)	Zero-pressure linewidth (MHz)	Pressure broadening (MHz/torr)
1	26	pure H	1399.474(46)	−2.97(42)	3.0(2)	9.0(1.5)
5	21	H in He mix	1399.562(69)	−0.69(37)	2.2(3)	5.7(1.4)
2	27	pure D	4240.695(62)	−3.86(55)		
3	14	pure D	4240.820(67)	−2.32(51)		
4	19	pure D	4240.696(57)	−1.55(49)	2.6(2)	6.0(1.3)
6	21	D in He mix			1.5(1)	4.5(0.7)

straight line for the line center frequency as a function of cell pressure. The $1S$-$2S$ cell fractured shortly after these sets of runs, so a new cell had to be made before more data could be collected. The installation of the cell resulted in the complete rebuilding and realignment of the $1S$-$2S$ spectrometer. Also, the dye in both lasers was changed and the lasers and the tellurium spectrometer were completely realigned. A new set of deuterium runs was then taken (set 3, 14 scans), giving a zero-pressure intercept consistent with that found from set 2, although the pressure shift was different. Similar runs the following day (set 4, 19 scans), gave results consistent with those of set 3. The pure deuterium gas bottle was then exchanged for a bottle containing a 5% H_2-5% D_2-90% He mixture (molecular %), and runs were taken on both the hydrogen (set 5, 21 scans) and deuterium (set 6, 21 scans) transitions.

3. *Signal magnitudes*

The largest absolute $1S$-$2S$ signal observed, 2.5×10^4 counts s^{-1}, was obtained with ~30 mW of 243-nm power and 200 mtorr of pure hydrogen in the cell, giving a linewidth of 2.5 MHz at 486 nm. The observed signal is about three orders of magnitude less than that expected from the assumptions of 100% dissociation and one detectable photon from every $2S$ atom created, the same factor observed by Hänsch *et al.*[5] We also found that in reducing the hydrogen concentration by a factor of 20 with the use of the helium mixture, the signal size only fell by a factor of 4.

It is important to note that even at cell pressures as low as 20 mtorr it was routinely possible to obtain peak count rates of 3000 s^{-1} on a statistical background of 1000 s^{-1}, so that the signal-to-noise ratio was not a limitation in the experiment.

B. Systematic shifts of $f(1S$-$2S)$

To assess the significance of the effects which give rise to systematic shifts of the transition, we note here that the uncertainty in our values for $f(1S$-$2S)$ and the $1S$ Lamb shift due to the frequency standards employed alone are of order 600 kHz. Note that all uncertainties quoted in this paper have the significance of one standard deviation.

1. *Pressure shift and broadening*

Figure 5 is a typical result for the pressure shift extrapolation. This graph is for pure hydrogen (set 1). The pressure dependence of the linewidth was obtained similarly. The results of this analysis are summarized in Table I.

The two intercepts for pure hydrogen are in good agreement with each other. A weighted mean of the two results gives the value 1399.500(38) MHz for the zero-pressure offset frequency. Unfortunately, a change in the temperature of the tellurium cell during the collection of the deuterium scans with the helium mixture (set 6) was accidentally overcompensated, rendering the center frequencies determined from these runs unreliable. The straight-line fit to these data is poor. However, the rejection of this data set is not a serious problem; we already have three independent sets of runs in pure deuterium, and the hydrogen results indicate that the measurements made with the helium mixture are consistent with those obtained in the pure gas. The agreement between the three deuterium intercepts is good. A weighted mean gives the final result 4240.732(35) MHz.

We believe that the major cause of the scatter in the values of the offset frequency recorded at a given pressure is the slow thermal fluctuations of the tellurium cell. The temperature of the cell wall was monitored and adjusted during the data collection, and the maximum observed

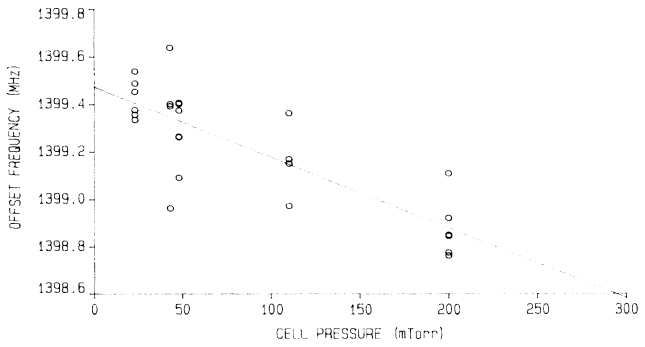

FIG. 5. Pressure shift extrapolation for data set 1. Each point is the raw center frequency of the $1S$-$2S$ line for a single run plotted against the cell pressure for that run. The line is an unweighted least-squares fit to all of the points.

fluctuations of ±4 °C suggest a limit on the frequency excursions of ±55 kHz (Sec. IV D 3), somewhat smaller than those seen in Fig. 5. However, the vapor pressure in the cell is of course determined by the temperature of the coldest point, in this case the cell windows. While the installation of the draught tubes certainly improved the cell stability, it is likely that the temperature changes of the windows were still larger than those of the lagged cell wall. The cell temperature was corrected on a time scale of about 100 s (the time between consecutive scans) so we expect that these fluctuations would average out over the considerably longer time spent collecting data at each pressure. The good agreement between the results of data sets made at different times confirms that this is indeed the case.

Although the zero-pressure intercepts of all three pure deuterium data sets are consistent, the pressure shift of set 2 appears to be anomalous. As the cell was only pumped for about an hour after changing the gas bottle, there may well have been some residual contamination of the vacuum system. This would have led to a different pressure shift, both directly and through a change in the dissociation fraction. In the analysis, we use the zero-pressure extrapolations from all three sets, but combine only the data of sets 3 and 4 to determine the pressure shift coefficient. A straight-line fit to the combined data set gives a pressure shift of −1.74(35) MHz/torr. The value we obtained above for hydrogen, −2.97(42) MHz/torr, is in good agreement with the result of −2.76(24) MHz/torr obtained by Beausoleil *et al.*[10] It is less precise because our data was taken at lower pressures than those used in the Stanford work, since we were more interested in the intercept than the slope. Finally, we note that the smaller shift for deuterium is in agreement with the result[38] (obtained from simple phase-shift theory) that the pressure shift decreases with velocity for interaction potentials that fall off faster than $1/r^3$, which is certainly the case for nonresonant broadening by collisions with molecules.

By combining the pressure broadening results for sets 1 and 4 with the respective pressure shifts found above, we calculated broadening-to-shift ratios of −3.0(9) for hydrogen and −3.4(1.4) for deuterium, consistent with the value of −2.8 expected for the van der Waals interaction.[38] The transit-time contribution to the linewidth[40] is 1.2 MHz for hydrogen and 0.85 MHz for deuterium (at 486 nm), so it is clear that the zero-pressure linewidth in these data sets contains a substantial contribution from the laser bandwidths. No firm conclusions can be drawn from the difference in the zero-pressure linewidth because these data sets were recorded several days apart, so the difference could just indicate a difference in the laser linewidths on the two days. However, the later runs using the helium mixture (sets 5 and 6) were all taken consecutively and the lasers were also operating considerably better for these runs. The linewidth at low pressure has a large contribution from the transit-time contribution for these data sets. The H-D difference in zero-pressure linewidth, 0.75(29) MHz, is in reasonable agreement with the calculated difference in the transit-time widths of 0.35 MHz.

2. dc Stark effect

Using second-order perturbation theory and including only the contribution from the nearby $2P_{1/2}$ level we estimate the shift of the $2S_{1/2}F=1$ level due to a weak electric field of strength E (V cm^{-1}) to be $4.7E^2$ kHz. The $1S$ shift is much smaller. Since there was no source of energetic ions in the apparatus, no special precautions were taken in this experiment to shield the interaction region from electric fields other than operating the photomultiplier with a grounded photocathode. A conservative upper limit on the stray electric field is 2 V cm^{-1}. This would correspond to a Stark shift of 19 kHz (at 122 nm), which is completely negligible compared to the other sources of error in this experiment.

3. ac Stark effect

There is also a level shift due to the 243-nm alternating electric field since two-photon transitions from an initial level to an intermediate level and then back to the initial level will give rise to diagonal matrix elements in second order.[41] The ac Stark shift of the transition frequency[42] is 1.67 I Hz in a linearly polarized field of intensity I (W cm^{-2}). In the present experiment the intensity at the center of the counterpropagating beams (each of 30-mW power and waist size 100 μm) was 380 W cm^{-2}. The total ac Stark shift is therefore 640 Hz which we can clearly ignore.

4. Zeeman effect

We now consider the perturbation of the $1S$ and $2S$ levels by a weak external magnetic field (in this context weak means that the level shift produced by the field is much less than the hyperfine splitting). Ignoring negligible relativistic effects, the g factor of both $1S$ and $2S$ levels is 1 for $F=1$, giving a level shift of $1.4m_F$ MHz/G. It follows from the two-photon transition selection rule $\Delta m_F=0$ that there is no shift in the frequency of any of the components of the $1S$-$2S$ transition. A similar result follows for deuterium which differs from hydrogen only in having nuclear spin $I=1$.

In view of this result no attempt was made to shield the interaction region from magnetic fields. The field was measured with a Hall probe and found to be 0(2) G, where the uncertainty comes solely from the sensitivity of the instrument. With a field of 2 G the level shift is 2.8 MHz, which is indeed much less than the hyperfine splittings of 1420 and 177 MHz in $1S$ and $2S$, respectively.

5. Second-order Doppler shift

The first-order Doppler shift is canceled in the absorption from the counterpropagating beams, but the second-order fractional Doppler shift $\frac{1}{2}(v/c)^2$ is not, so it is necessary to lower the laser frequency by this amount to obtain resonance with the moving atom. If all atoms contributed equally to the total two-photon absorption signal, then the shift could be found by simply substituting the mean-square thermal velocity $v^2=3$ kT/M into

this expression. This gives shifts of 102 kHz for hydrogen and 51 kHz for deuterium (at 122 nm). However, in our case slower atoms contribute a proportionately larger fraction of the total two-photon signal since they spend longer in the interaction region, so the actual shift will be somewhat less than this. The shift could obviously be calculated by making a numerical integration of the transition probability over the thermal velocity distribution, but since it has a negligible effect on our final result we simply use these values with a 100% uncertainty to indicate that they are an upper bound for the second-order Doppler shift.

6. Amplitude modulation

The effect of the amplitude modulation of the reference laser is analyzed in detail elsewhere.[13] It has the effect of mixing in a small amount of the symmetric saturated absorption line shape into the first derivative error signal. For a line of FWHM Γ the shift is $(\epsilon/\delta)\Gamma^2/4$ for frequency modulation of depth δ (5 MHz here) and fractional intensity modulation ϵ. The intensity modulation was monitored throughout the data collection, and did not exceed 0.4%. The sign of the amplitude modulation changed with time, presumably as the lock point of the dye laser to its intracavity étalon moved. We therefore take the value of the correction (at 486 nm) as 0(80) kHz for hydrogen and 0(40) kHz for deuterium. The deuterium contribution is smaller because the tellurium b_1 line is narrower.

7. Servo offsets

Offsets in the tellurium servo-lock were checked and nulled frequently during the data collection; we can place an upper bound of 10 kHz (at 486 nm) on shifts arising from this source.

8. Hyperfine structure

The hyperfine structure produces a negligible change in the centroid of the $1S$-$2S$ transition. We therefore correct for it by simply adding $\frac{7}{32}$ of the hydrogen ground-state hyperfine splitting[43] ($\frac{7}{24}$ for deuterium) to obtain the centroid.

9. Acousto-optic modulator

Since the acousto-optic modulator upshifted the pump beam in the tellurium saturation spectrometer by 40.000 MHz, a correction of 20.000 MHz in the peak position is required.

C. Determination of $f(1S$-$2S)$

Table II summarizes the reduction of our measured values of $f(1S$-$2S)/4-f(Te)$ to obtain $f(1S$-$2S)$ including the systematic corrections discussed above.

In calculating the values given for f(Te), the frequency of the appropriate tellurium calibration line, we have made use of the ratios of tellurium transition frequencies to the He-Ne standard laser frequency determined in the original calibration.[35] The frequency used for the NPL iodine-stabilized He-Ne laser has been taken as that calculated from the direct frequency measurement of the National Bureau of Standards U.S. (NBS) standard laser[44] and the known NPL-NBS standard laser frequency difference[45] of +38(22) kHz.

D. Determination of the 1S Lamb shift

To determine a value for the $1S$ Lamb shift (Table III) from the measured $1S$-$2S$ transition frequency $f_{\text{expt}}(1S$-$2S)$, we first subtract off $f_D(1S$-$2S)$, the interval given by the difference of the Dirac energy levels, calculated using $R_\infty = 109\,737.315\,714(19)\ \text{cm}^{-1}$ (a weighted mean of the two most precise values[46,47]). We also add on the known $2S_{1/2}$ Lamb shift (obtained from the measured value of the $2S_{1/2}$-$2P_{1/2}$ interval[2,3,48] and the theoretical value for the small $2P_{1/2}$ Lamb shift[18]) and the correction for the relativistic effects of nuclear motion [Eq. (2)]. Our definition of the Lamb shift is the same as that of Johnson and Soff,[15] i.e., the sum of all QED contributions plus the correction for finite nuclear size.

There is a direct link between our measurement of $f(1S$-$2S)$ at Oxford and the recent measurements of the Rydberg constant made by Zhao *et al.* at Yale Universi-

TABLE II. Determination of the $1S$-$2S$ transition frequency.

	Hydrogen		Deuterium	
	Frequency (MHz)	Error (MHz)	Frequency (MHz)	Error (MHz)
Measured offset frequency	1399.50	0.04	4240.73	0.04
Hyperfine-structure correction	77.68		23.87	
Acousto-optic modulator	−20.00		−20.00	
Amplitude modulation	0.00	0.08	0.00	0.04
Second-order Doppler shift	0.03	0.03	0.01	0.01
Servo offsets, etc.	0.00	0.01	0.00	0.01
$f_{\text{expt}}(1S$-$2S)/4-f$(Te)	1457.20	0.09	4244.62	0.06
$4[f_{\text{expt}}(1S$-$2S)/4-f$(Te)]	5 828.82	0.37	16 978.47	0.22
$4f$(Te)	2 466 055 585.30	0.66	2 466 715 429.98	0.66
$f_{\text{expt}}(1S$-$2S)$	2 466 061 414.12	0.75	2 466 732 408.45	0.69

TABLE III. Determination of the $1S$ Lamb shift. The asterisk means that the uncertainty in the frequency of the NBS standard laser contributes 1.6 parts in 10^{10} to each $1S$-$2S$ frequency, but cancels out in the small difference frequency (see discussion in text).

	Hydrogen		Deuterium	
	Frequency (MHz)	Error (MHz)	Frequency (MHz)	Error (MHz)
$f_{\text{expt}}(1S\text{-}2S)$	2 466 061 414.12	0.75	2 466 732 408.45	0.69
$f_D(1S\text{-}2S)$	2 466 068 519.36	0.46	2 466 739 534.56	0.46
$f_{\text{expt}}(1S\text{-}2S)-f_D(1S\text{-}2S)$	7105.24	0.69*	7126.11	0.63*
$+2S_{1/2}$-$2P_{1/2}$ Lamb shift	1057.85	0.01	1059.28	0.06
$+2P_{1/2}$ Lamb shift	−12.83		−12.83	
$+2S$-$1S$ two-body correction	22.33		11.18	
$1S$ Lamb shift	8172.58	0.69	8183.74	0.63

ty[46] and Biraben *et al.* at l'Ecole Normale Supérieure, Paris.[47] We have measured $f(1S\text{-}2S)$ relative to a tellurium cell which has itself been calibrated against an NPL He-Ne standard laser, and this NPL laser has been directly compared with an NBS He-Ne standard laser on two separate occasions. Zhao *et al.* calibrated their experiment with an NBS He-Ne standard laser, and Biraben *et al.* measured the Rydberg constant relative to a He-Ne laser at the Bureau International des Poids et Mesures (BIPM) which can also be traced back to the NBS laser. Therefore the frequency of the standard He-Ne laser is an overall scale factor for both our measured $1S$-$2S$ frequency $f_{\text{expt}}(1S\text{-}2S)$ and the calculated Dirac $1S$-$2S$ interval $f_D(1S\text{-}2S)$. It follows that while the small difference of these two intervals is sensitive to the difference in the frequencies of the NPL and NBS standard lasers [and this is already included in f(Te) in Table I], it is quite insensitive to the absolute frequency of the standard laser. Accordingly, we can reduce the uncertainty in the calculated Lamb shift to take account of the cancelation of the 1.6 parts in 10^{10} systematic uncertainty (equivalent to 385 kHz) that the He-Ne frequency contributes to both $f_{\text{expt}}(1S\text{-}2S)$ and $f_D(1S\text{-}2S)$.

Our experimental values, 8172.6(7) MHz for hydrogen and 8183.7(6) MHz for deuterium, are in excellent agreement with the theoretical results of 8173.03(9) MHz and 8184.08(12) MHz, respectively. The hydrogen result is a factor of 3 more precise than the recent Stanford cw measurement,[10] mainly because the calibration was more direct. The deuterium measurement is the first result for this isotope obtained by cw methods, and is a factor of 50 more precise than the previous best value.[6] The various sources of uncertainty in our results are summarized in Table IV and our measurement is compared with other measurements of the $1S$ Lamb shift in Table V.

E. Rydberg constant

If we assume that the state dependence of the Lamb shift is understood, an alternative interpretation of the measurement is possible. We can use the theoretical value of the $1S$ Lamb shift with the other quantities appearing in Table III to calculate a value for $f_D(1S\text{-}2S)$, and so obtain a value for the Rydberg constant. This reduction is summarized in Table VI, and the sources of uncertainty are listed in Table VII. The most recent values of the fundamental constants[49] required in the calculation were used.

Our final value of $R_\infty = 109\,737.315\,73(3)\ \text{cm}^{-1}$ is in excellent agreement with other recent measurements (Table VIII). Note that the $1S$ Lamb shift would have to be wrong by more than six times its estimated uncertainty to affect our result significantly, so our assumption that the theoretical value of the $1S$ Lamb shift is correct is not very strict.

In Tables II to VI we have taken the frequency of a He-Ne laser locked to component "i" of the 11-5 $R(127)$ transition in $^{127}I_2$ as that given by the result of the single

TABLE IV. Contributions to the uncertainty in the measured $1S$ Lamb shift.

	Hydrogen (kHz)	Deuterium (kHz)
Zero-pressure intercept	152	140
Amplitude modulation	320	160
Servo offsets	40	40
Second-order Doppler shift	102	51
$2S_{1/2}$-$2P_{1/2}$ Lamb shift (expt)	9	64
Te to He-Ne frequency ratio	518	518
Rydberg constant to He-Ne frequency ratio	235	235
NPL-NBS He-Ne difference	114	114
Total (rms error)	688	625

TABLE V. Measurements of the 1S Lamb shift by laser spectroscopy. Where necessary, results have been corrected for the latest measurements of the Rydberg constant (Refs. 46 and 47) and the relativistic two-body correction has been subtracted to make the results consistent with the definition of the Lamb shift used in this paper.

Reference	1S Lamb shift (MHz)	Error (MHz)	243-nm source	Frequency calibration
Hydrogen				
Hänsch *et al.*[a]	8600	800	pulsed	Doppler-broadened absorption spectroscopy of Balmer β
Lee *et al.*[b]	8220	100	pulsed	saturated absorption spectroscopy of Balmer β
Wieman and Hänsch[c]	8175	30	pulsed	polarization spectroscopy of Balmer β
Hildum *et al.*[d]	8191.1	5.4	pulsed	saturated absorption spectroscopy of tellurium
Barr *et al.*[e]	8190	25	pulsed	saturated absorption spectroscopy of tellurium
McIntyre *et al.*[f]	8173.50	1.9	cw	saturated absorption spectroscopy of tellurium
This work	8172.6	0.7	cw	saturated absorption spectroscopy of tellurium
Theory	8173.03	0.09		
Deuterium				
Hänsch *et al.*[a]	8300	300	pulsed	Doppler-broadened absorption spectroscopy of Balmer β
Lee *et al.*[b]	8260	110	pulsed	saturated absorption spectroscopy of Balmer β
Wieman and Hänsch[c]	8189	30	pulsed	polarization spectropy of Balmer β
This work	8183.7	0.6	cw	saturated absorption spectroscopy of tellurium
Theory	8184.08	0.12		

[a]Reference 5.
[b]Reference 4.
[c]Reference 6.
[d]Reference 7.
[e]Reference 8.
[f]Reference 10.

measurement made at the NBS;[44] this result has an uncertainty of 1.6 parts in 10^{10}. If instead, we use value recommended by the Comité Consultatif pour la Définition Du Mètre,[52] with its larger 3.4 parts in 10^{10} uncertainty, our value of the Rydberg constant changes from 109 737.315 731(31) cm^{-1} to 109 737.315 725(45) cm^{-1}. Our values for the 1S Lamb shift are unaffected by this; the Lamb shift is sensitive only to the frequency difference between the NPL and NBS standard He-Ne lasers.

The dominant source of error in our Rydberg constant determination is again the tellurium calibration (Table VI). Unfortunately, the uncertainty in the best frequency measurement of the standard helium-neon laser limits the possibility for improving the precision by more than a factor of 2 (this limit has, in fact, been reached in the most precise of the recent measurements[47]). A better visible frequency standard will thus be required if this aspect of our experiment is to be improved. Alternatively, if a better value of the Rydberg constant can be determined, e.g., by microwave spectroscopy of circular Rydberg states,[53] then 1S-2S and other transitions in the hydrogen atom could be used to realize the meter in the visible and ultraviolet region of the spectrum.[54]

F. H-D 1S-2S isotope shift

We note finally that the value of the H-D 1S-2S isotope shift obtained from these measurements, 670 994.33(64) MHz, is in excellent agreement with the calculated value of 670 994.39(12) MHz. The precision is insufficient to give any useful information about either the proton and deuteron charge radii or the electron-proton mass ratio m_e/M_p, but it is still a valuable consistency check on both our measurements and the tellurium calibration.

V. CONCLUSIONS

This paper has described the first spectroscopic studies of the hydrogen 1S-2S transition made using cw 243-nm

TABLE VI. Determination of the Rydberg constant.

	Hydrogen		Deuterium	
	Frequency (MHz)	Error (MHz)	Frequency (MHz)	Error (MHz)
$f_{expt}(1S\text{-}2S)$	2 466 061 414.12	0.75	2 466 732 408.45	0.69
$+1S$ Lamb shift (theory)	8173.03	0.09	8184.08	0.12
$-2S\text{-}1S$ two-body correction	−22.33		−11.18	
$-2S_{1/2}\text{-}2P_{1/2}$ Lamb shift	−1057.85	0.01	−1059.28	0.06
$-2P_{1/2}$ Lamb shift	12.83		12.83	
$f_D(1S\text{-}2S)$	2 466 068 519.81	0.76	2 466 739 534.90	0.71
R_∞	109 737.315 734(34) cm^{-1}		109 737.315 729(31) cm^{-1}	
Average R_∞	109 737.315 731(31) cm^{-1}			

TABLE VII. Contributions to the uncertainty in the Rydberg constant.

	Hydrogen (parts in 10^{11})	Deuterium (parts in 10^{11})
Zero-pressure intercept	6	6
Amplitude modulation	13	6
Servo offsets	2	2
Second-order Doppler shift	4	2
$2S_{1/2}$-$2P_{1/2}$ Lamb shift (expt)	0	3
Te to He-Ne frequency ratio	22	22
NBS He-Ne frequency standard	16	16
$1S$ Lamb shift (theory)	4	5
Total (rms error)	31	29

light generated by frequency doubling. The experiment has improved the precision of the $1S$ Lamb shift in hydrogen by a factor of 3, to 8 parts in 10^5. The result obtained is in excellent agreement with theory. An alternative interpretation of the measurements gives a value for the Rydberg constant with an uncertainty of 3 parts in 10^{10}.

In the course of this work three crystals have been investigated for second-harmonic generation of the cw 243-nm light. β-barium borate has been found to be superior to both urea and lithium formate monohydrate because it is available in crystals of excellent optical quality and because it is not damaged by uv generation. Its only disadvantage is the large walkoff distortion of the generated uv beam but we have found that this can be described theoretically and largely compensated for. Using a BBO crystal inside the cavity of a ring dye laser we were routinely able to generate 3 mW of cw 243-nm light which was further increased by a factor of 12 in an enhancement cavity.

An exciting result of this work is the potential now offered for making a large improvement in the precision of the $1S$ Lamb shift. The present experiment has been calibrated by comparing the $1S$-$2S$ transition observed at Oxford University with other hydrogen transitions observed at Yale and l'Ecole Normale Supérieure; the uncertainties introduced by the intermediate stages in this chain are the factors limiting the precision of our Lamb shift measurement. In the next development the direct comparison described in the introduction will be realized by replacing the tellurium spectrometer with a Balmer-β spectrometer. The transition will be excited in a beam of metastable $2S_{1/2}$ atoms, to provide high resolution and to avoid the perturbing effects of collisions and the electric fields that would be encountered in a discharge. The two transitions can, of course, be directly compared by heterodyning. A factor of 2 improvement would be obtained by simply calibrating the $1S$-$2S$ transition against the $2S$-$4P$ transition, the allowed transition used in the Yale experiment. However, there exist a number of possibilities that allow observation of the narrow ($\sim$1 MHz) $2S$-$4S$ transition: a small static electric field, a two-photon transition using optical, and rf photons[55,56] or a two-photon transition using two 972-nm optical photons. These methods are now being investigated. It is expected that it should then be possible to compare the two transition frequencies to much higher precision. In the experiment described in this paper the center of the $1S$-$2S$ resonance was located to 150 kHz. However, this error is dominated by the statistical contribution that arose from fluctuations in the temperature of the tellurium cell and so it should be much smaller when a better reference is used. It thus should be possible to compare the two transitions to a precision approaching 40 kHz. This optical measurement would then test the QED corrections in hydrogen with an uncertainty of 1 part in 10^5, a precision comparable to that of the best radio-frequency measurements of the $2S_{1/2}$ Lamb shift. At this level of precision the discrepancy in the measurements of the proton size becomes important. One possible way around this difficulty is to compare the $2S$-$4S$ transition of the He^+ ion with the $1S$-$2S$ transition in hydrogen. The increase in Z emphasizes the higher-order corrections that provide the calculational difficulty in the Lamb shift. Further, the α-particle radius is known precisely, both from direct electron scattering measurements[57] and from a measurement of the fine-structure interval in muonic helium.[58] The two comparisons H($1S$-$2S$)-4H($2S$-$4S$) and H($1S$-$2S$)-He^+($2S$-$4S$) would then determine both the QED corrections and the proton size. The application of the two-photon technique to He^+ is currently being investigated by two of us.[59]

TABLE VIII. Recent measurements of the Rydberg constant.

Reference	Rydberg constant (cm^{-1})
McIntyre *et al.*[a]	109 737.315 69(8)
Zhao *et al.*[b]	109 737.315 69(7)
Biraben *et al.*[c]	109 737.315 69(6)
Zhao *et al.*[d]	109 737.315 73(3)
Biraben *et al.*[e]	109 737.315 709(18)
This work	109 737.315 73(3)

[a]Reference 10.
[b]Reference 50.
[c]Reference 51.
[d]Reference 46.

ACKNOWLEDGMENTS

It is a pleasure to acknowledge the very skillful efforts of S. H. Smith and G. Read of the Clarendon Laboratory

in respectively growing and polishing the high-quality urea crystals which were essential to the development of this experiment. The expert technical assistance and dedication of C. W. Goodwin and S. Giles were also important elements in this work. We thank A. I. Ferguson for the loan of the calibrated tellurium cell. One of us (M.G.B.) is pleased to acknowledge the support of the Royal Commission for the Exhibition of 1851, the New Zealand University Grants Committee and Christ Church, Oxford. One of us (C.J.F.) receives support from the Royal Society. This work was supported by grants from the Science and Engineering Research Council, which also gave additional support to M.D.P., D.A.T., E.A.H., and D.N.S. We have profited from discussions and practical help from many colleagues, particularly M. H. Dunn and C. W. P. Palmer.

---

*Present address: Department of Physics, Yale University, New Haven, CT 06520.

†Permanent address: Department of Physics, Yale University, New Haven, CT 06510.

‡Permanent address: Department of Physics, University of Western Australia, Nedlands, Western Australia 6009, Australia.

§Present address: Department of Physics, University of Virginia, Charlottesville, VA 22901.

**Permanent address: Department of Physics, University of Otago, P.O. Box 56, Dunedin, New Zealand.

[1]E. V. Baklanov and V. P. Chebotayev, Opt. Commun. **12**, 312 (1974); E. V. Baklanov and V. P. Chebotayev, Opt. Spectrosc. **38**, 215 (1975).

[2]S. R. Lundeen and F. M. Pipkin, Phys. Rev. Lett. **46**, 232 (1981).

[3]V. G. Pal'chikov, Yu. L. Sokolov, and V. P. Yakovlev, Metrologia **21**, 99 (1985).

[4]S. A. Lee, R. Wallenstein, and T. W. Hänsch, Phys. Rev. Lett. **35**, 1262 (1975).

[5]T. W. Hänsch, S. A. Lee, R. Wallenstein, and C. Wieman, Phys. Rev. Lett. **34**, 307 (1975).

[6]C. Wieman and T. W. Hänsch, Phys. Rev. A **22**, 192 (1980).

[7]E. A. Hildum, U. Boesl, D. H. McIntyre, R. G. Beausoleil, and T. W. Hänsch, Phys. Rev. Lett. **56**, 576 (1986).

[8]J. R. M. Barr, J. M. Girkin, J. M. Tolchard, and A. I. Ferguson, Phys. Rev. Lett. **56**, 580 (1986).

[9]C. J. Foot, B. Couillaud, R. G. Beausoleil, and T. W. Hänsch, Phys. Rev. Lett. **54**, 1913 (1985).

[10]R. G. Beausoleil, D. H. McIntyre, C. J. Foot, B. Couillaud, E. A. Hildum, and T. W. Hänsch, Phys. Rev. A **35**, 4878 (1987); D. H. McIntyre, R. G. Beausoleil, C. J. Foot, E. A. Hildum, B. Couillaud, and T. W. Hänsch, *ibid.* **39**, 4591 (1989).

[11]C. J. Foot, P. E. G. Baird, M. G. Boshier, D. N. Stacey, and G. K. Woodgate, Opt. Commun. **50**, 199 (1984).

[12]Preliminary results from this work were reported in M. G. Boshier, P. E. G. Baird, C. J. Foot, E. A. Hinds, M. D. Plimmer, D. N. Stacey, J. B. Swan, D. A. Tate, D. M. Warrington, and G. K. Woodgate, Nature **330**, 463 (1987). The small differences between the results given in that paper and those presented here are mainly due to the use of an updated value for the Rydberg constant.

[13]M. G. Boshier, D. Phil. thesis, University of Oxford, 1988 (unpublished).

[14]G. W. Erickson, J. Phys. Chem. Rev. Data **6**, 831 (1977).

[15]W. R. Johnson and G. Soff, At. Data Nucl. Data Tables **33**, 405 (1985).

[16]P. J. Mohr, Phys. Rev. Lett. **34**, 1050 (1975).

[17]G. Bhatt and H. Grotch, Phys. Rev. **A31**, 2794 (1985); G. Bhatt and H. Grotch, Phys. Rev. Lett. **58**, 471 (1987); G. Bhatt and H. Grotch, Ann. Phys. (New York) **178**, 1 (1987).

[18]G. W. Erickson and H. Grotch, Phys. Rev. Lett. **60**, 2611 (1988).

[19]G. G. Simon, Ch. Schmitt, F. Borkowski, and V. H. Walther, Nucl. Phys. A **333**, 381 (1980).

[20]T. E. O. Ericson, Nucl. Phys. A **416**, 281c (1984).

[21]L. S. Vasilenko, V. P. Chebotayev, and A. V. Shishaev, JETP Lett. **12**, 113 (1970) [Pis'ma Zh. Eksp. Teor. Fiz. **12**, 161 (1970)].

[22]B. Cagnac, G. Grynberg, and F. Biraben, J. Phys. **34**, 84 (1973).

[23]F. Bassani, J. J. Forney, and A. Quattropani, Phys. Rev. Lett. **39**, 1070 (1977).

[24]M. Glass-Maujean, Phys. Rev. Lett. **62**, 144 (1989).

[25]G. Grynberg and B. Cagnac, Rep. Prog. Phys. **40**, 791 (1977).

[26]Chen Chuangtian, Wu Bochang, Jiang Aidong, and You Guiming, Sci. Sin B **28**, 235 (1985).

[27]K. Kato, IEEE J. Quantum Electron. **QE-22**, 1013 (1986).

[28]J. Slevin and W. Stirling, Rev. Sci. Instrum. **52**, 1780 (1981).

[29]W. W. MacAlpine and R. O. Schildknecht, Proc. IRE **47**, 2099 (1959).

[30]H. C. Berg and D. Kleppner, Rev. Sci. Intrum. **33**, 248 (1962).

[31]J. T. M. Walraven and I. F. Silvera, Rev. Sci. Instrum. **53**, 1167 (1982).

[32]K. C. Harvey and C. Fehrenbach, Jr., Rev. Sci. Instrum. **54**, 1117 (1983).

[33]M. Born and E. Wolf, *Principles of Optics* (Pergamon, New York, 1959).

[34]G. D. Boyd, A. Ashkin, J. M. Dziedzic, and D. A. Kleinman, Phys. Rev. **137**, A1305 (1965).

[35]J. R. M. Barr, J. M. Girkin, A. I. Ferguson, G. P. Barwood, P. Gill, W. R. C. Rowley, and R. C. Thompson, Opt. Commun. **54**, 217 (1985); J. R. M. Barr, Ph.D. thesis, University of Southampton, 1987 (unpublished).

[36]D. H. McIntyre and T. W. Hänsch, Phys. Rev. A **34**, 4504 (1986).

[37]D. Bebelaar, Rev. Sci. Instrum. **50**, 1629 (1979).

[38]A. Corney, *Atomic and Laser Spectroscopy* (Oxford University, New York, 1977).

[39]W. H. Press, B. P. Flannery, S. A. Teukolsky, and W. H. Vetterling, *Numerical Recipes* (Cambridge University, Cambridge, England, 1986).

[40]F. Biraben, M. Bassini, and B. Cagnac, J. Phys. **40**, 29 (1977).

[41]A. M. Bonch-Bruevich and V. A. Khodovi, Sov. Phys. Usp. **85**, 3 (1967) [Usp. Fiz. Nauk **93**, 71 (1967)].

[42]A calculation by S. Chu is reported in R. G. Beausoleil and T. W. Hänsch, Phys. Rev. A **33**, 1661 (1986).

[43]P. Kusch, Phys. Rev. **100**, 1188 (1955).

[44]D. A. Jennings, C. R. Pollock, F. R. Petersen, R. E. Drullinger, K. M. Evenson, J. S. Wells, J. L. Hall, and H. P. Layer, Opt. Lett. **8**, 136 (1983).

[45]H. P. Layer, W. R. C. Rowley, and B. R. Marx, Opt. Lett. **6**, 188 (1981); W. R. C. Rowley (private communication); H. P. Layer (private communication).

[46]P. Zhao, W. Lichten, H. P. Layer, and J. C. Bergquist, Phys. Rev. Lett. **58**, 1293 (1987).
[47]F. Biraben, J. C. Garreau, L. Julien, and M. Allegrini, Phys. Rev. Lett. **62**, 621 (1989).
[48]B. L. Cosens, Phys. Rev. **49**, 173 (1968).
[49]E. R. Cohen and B. N. Taylor, Rev. Mod. Phys. **59**, 1121 (1987).
[50]P. Zhao, W. Lichten, H. P. Layer, and J. C. Bergquist, Phys. Rev. A **34**, 5138 (1986).
[51]F. Biraben, J. C. Garreau, and L. Julien, Europhys. Lett. **2**, 925 (1986).
[52]See the documents concerning the new definition of the metre, Metrologia **19**, 163 (1983).
[53]J. Liang, M. Gross, P. Goy, and S. Haroche, Phys. Rev. A **33**, 4437 (1986).
[54]P. Zhao, W. Lichten, H. P. Layer, and J. C. Bergquist, in *Laser Spectroscopy VIII,* edited by W. Persson and S. Svanberg (Springer-Verlag, Berlin, 1987).
[55]D. E. Roberts and E. N. Fortson, Phys. Rev. Lett. **31**, 1539 (1973).
[56]D. Shiner and C. Wieman, *Precision Measurements and Fundamental Constants II,* Natl. Bur. Stand. (U.S.) Spec. Publ. No. 617, edited by B. N. Taylor and W. D. Phillips (U.S. GPO, Washington, D.C., 1984).
[57]I. Sick, Phys. Lett. **116B**, 212 (1982).
[58]E. Borie and G. A. Rinker, Phys. Rev. A **18**, 324 (1978).
[59]M. G. Boshier and E. A. Hinds (unpublished).